

Ultrafast T-Jump in Water: Studies of Conformation and Reaction Dynamics at the Thermal Limit

Hairong Ma, Chaozhi Wan, and Ahmed H. Zewail*

Physical Biology Center for Ultrafast Science and Technology, and Laboratory for Molecular Sciences, California Institute of Technology, Pasadena, California 91125

Received February 27, 2006; E-mail: zewail@caltech.edu

Almost all biological reactions occur in water and thermally at room temperature. To monitor the evolution of conformational change and reactivity in such a matrix, a triggering “heat jump”, which is faster than the change itself, is required. On the microsecond time scale, this T-jump can be achieved using the relaxation method.¹ With lasers, the nanosecond time scale can be achieved and has been used with great success in the studies of fast kinetics of, for example, protein folding.^{2,3} Typically, a Raman shifted Nd:YAG laser is used to heat the solution (H₂O or D₂O), and the pulse duration is ~10 ns. Although, in some cases, a 50 ps pulse was used, the kinetics resolved is on the nanosecond time scale.⁴ To achieve shorter time resolution than nanoseconds, dye molecules have been invoked as a heating media between solvent and solute molecules (e.g., proteins), and ~70 ps or longer resolution was reported; see, for example, refs 5–7. Because of the possible dye–solute interaction, care has to be taken to deconvolute any contribution to the dynamics from that of the dye itself. More importantly, the energy transfer process from the dye molecules, via the solvent, to the solute molecules limits the time resolution.

Here, we report the development of ultrafast T-jump, directly in water and with time resolution reaching the fundamental time scale of water thermalization,⁸ through hydrogen bonding, namely, ~5 ps. The T-jump heats the water via the overtone absorption of the OH– stretch at 1.5 μm . Using a new design for overlap geometry and focusing, and pulse stretching techniques, we are able to routinely increase the temperature of bulk water by up to 20 $^{\circ}\text{C}$, but maintain the ultrafast time resolution, as described below. This achievement is nontrivial in view of the fact that pulses of femtosecond duration have large peak power and can induce white-light continuum generation. We demonstrate the methodology reported here first for the studies of large molecules binding (recognition) in water and for conformational changes. The results indicate the ability to resolve the distinct time scales of solvation (a few picoseconds), conformational changes (hundreds of picoseconds), and binding (nanoseconds). We also studied water exchange reactions involving metal coordination and the initial steps of “melting” of DNA. For reactions, the stepwise hydration was resolved, and for DNA, the dynamics of premelting was observed.

The experimental setup is schematically illustrated in Figure 1. The pulses were generated by two OPA systems pumped by a Ti:sapphire amplifier with a repetition rate of 200 Hz. The T-jump pulse was set to 1.45 μm with a typical energy of 15 μJ , stretched to 5–20 ps. The time-delayed probe pulse (~100 fs) has much less energy (<1 nJ) and was tuned to different wavelengths to monitor changes of interest. The sample was held in a 100 or 300 μm thick flat capillary cell and was placed in a temperature-controlled cell holder with minimal disturbance of alignment.

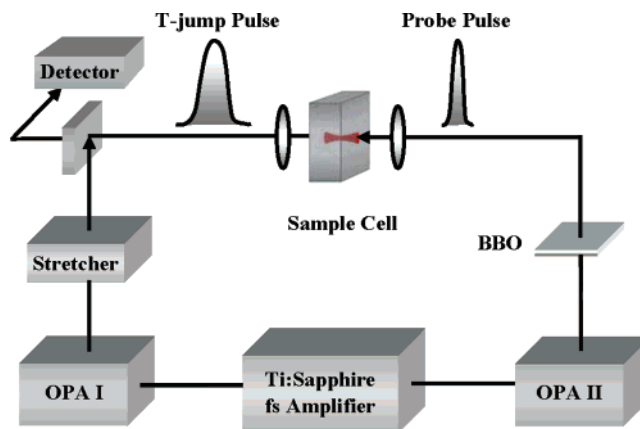


Figure 1. Schematic diagram of the ultrafast laser T-jump.

Numerous control experiments were performed to ensure reproducibility and generality of the approach.

We monitored the temperature jump in pure water with the probe wavelength being at 1.55 μm . By knowing the change of absorbance as a function of temperature (both transient and steady state), we determine the temperature increase, ΔT . Water absorption is very sensitive to temperature changes, and the observed negative absorbance in Figure 2 (left) gives a ~7 $^{\circ}\text{C}$ T-jump in the 300 μm thick cell; higher temperatures were achieved in the 100 μm thick cell. Following the T-jump, thermal equilibration in bulk water is reached in ~5 ps,⁸ and this limit of ultrafast relaxation is due to the high density of the low-frequency modes provided by the hydrogen bond network.⁹ It should be noted that the heating pulse jumps the temperature of water molecules in the heated volume and water remains hot for the longest delay time used (4.8 ns) since diffusion of heat from this microns size volume to cold bulk water occurs on tens of microseconds. With millisecond pulse repetition, every heating pulse repeats the experiment on water at the initial temperature.

We applied the methodology to various molecular systems, chemical and biological. First, here we detail the case for probing thermal association and conformational changes of xanthene derivative, rhodamine 6G (R6G). In aqueous solution, it aggregates to form dimers^{10,11} and the absorption peak of the monomer at 527 nm shifts to 500 nm upon dimerization. The blue shift, in an excitonic description, indicates that the dimer molecules acquire an “H” geometry, where the two molecules lie in nearly parallel planes with a calculated interplanar distance of 3.5 \AA .¹² The increase in the intensity of the monomer band with increasing temperature, accompanied by the decrease in the intensity of the dimer band, is a signature of dissociation: the equilibrium shifts toward the monomer state when the temperature increases.

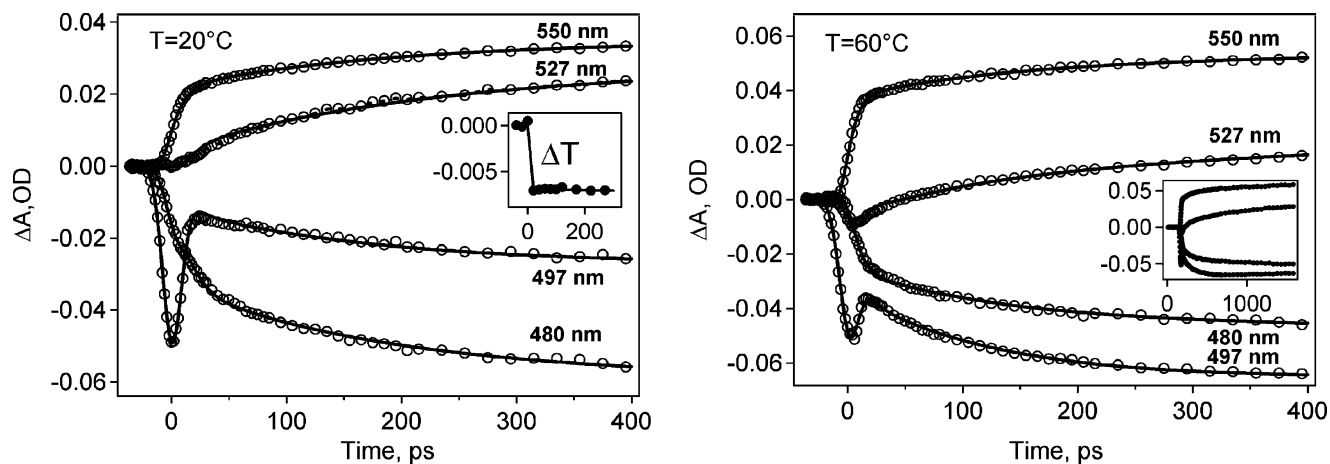


Figure 2. Transient absorption of R6G induced by T-jump: (○) experimental data; (—) theoretical fits with a global multiexponential model convoluted with a Gaussian response function, including another component for the nonlinear response (peak at 497 nm). (Left) Relaxation initiated at 20 °C. Inset: T-jump monitored by absorption change of water. (Right) Relaxation initiated at 60 °C. Inset: long time dynamics.

Scheme 1. Bimolecular Association at Equilibrium, with k_a and k_d Noted

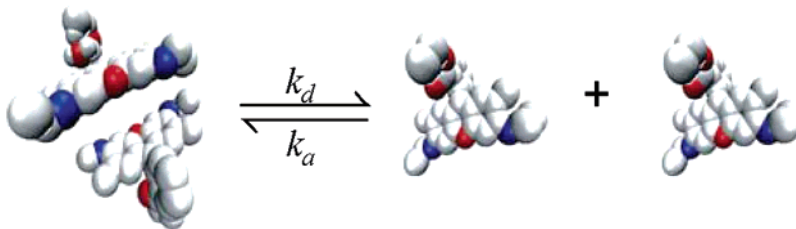
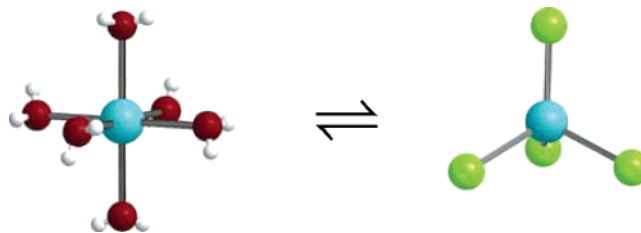


Figure 2 presents the time-resolved transient absorption change of R6G solution pre-equilibrated at 20 and 60 °C at wavelengths of 480, 497, 527, and 550 nm. The transients were taken at the magic angle (54.7°) in order to avoid the influence of rotational motion. Global fitting of all the transients with different wavelengths at a fixed temperature shows that three distinctive time scales are involved: at 20 °C, 11 ps (τ_1); 150 ps (τ_2); and 30 ns (τ_3). The lifetime τ_3 is a rough estimation because of the short time window (1.6 ns) used in this case. At a higher temperature (60 °C), τ_1 and τ_2 decrease to 6 and 100 ps, respectively, while τ_3 reduces significantly to 2 ns. Because of limits on thermalization and resolution times, τ_1 could even be shorter. We also studied the transient behavior when the polarization of the T-jump and probe pulses was either parallel or perpendicular. We clearly see the transient anisotropy. In this case, the anisotropy is due to the induced orientation by the electric field. We note the contrast with conventional dipole anisotropy,¹³ as here the initial orientation must be carried through the solvent, water.

The ultrafast component (τ_1) is robust for both monomer and dimer, and in our analysis (Figure 2), it is a “desolvation” process as hydrogen bonding with the positively charged R6G must change with temperature. This is supported by the observed spectral change of the monomer steady state absorption.¹⁴ For the dimer, this ultrafast process is followed by conformational change into an intermediate structure, prior to dissociation. Thus τ_2 reflects this change, and it is not surprising that such a large pair will have to first adjust to a modified structure when the temperature increases prior to final departure of monomers. MD simulations predict two conformations, but NMR, on its time scale, suggests one.¹² Temperature-induced partial unfolding was deduced for similar systems from steady state measurements.¹⁵ The fact that the rotation time constant of R6G is on the time scale of τ_2 ¹⁶ further support the change in conformation.

In water, the aggregation of two monomers to form a dimer must be a bimolecular reaction (Scheme 1), with k_d and k_a determining the equilibrium constant. The observed rate constant, which is $k_{\text{obs}} \approx 4k_a c + k_d$, can be estimated from knowledge of k_a (using the Smolochowski theory) and k_d (from the equilibrium constant). We obtained for a total concentration of 5 mM an equilibrium constant of 1000 M⁻¹ and a relaxation time of 20 ns at 20 °C in water, which reproduces the observed range of τ_3 at room temperature. All essential features of the experimental results, τ_1 , τ_2 , and τ_3 and their components, are reproduced with the kinetics model describing desolvation, conformational change, and dimerization.

Scheme 2. The Two Structures Involved in Ligand Substitution Reactions in Water



For ligand–water exchange reactions (Scheme 2), we focused our attention on the classic case of ligand ($X = \text{Cl}^-$ or Br^-) substitution reactions of hydrated cobalt complexes $[\text{CoX}_i(\text{H}_2\text{O})]^{2-i}$. We resolved the elementary steps, which occur on different time scales, and for different temperatures (Figure 3). As the complex structure changes from being octahedral to being tetrahedral,¹⁷ the absorption spectra change. For a given T-jump, we observed the ligand exchange on the time scale in the range of a few picoseconds, 20 and 300 ps, and several nanoseconds. As noted in Figure 3, the experiments with D₂O give the predicted scaling of signal, based

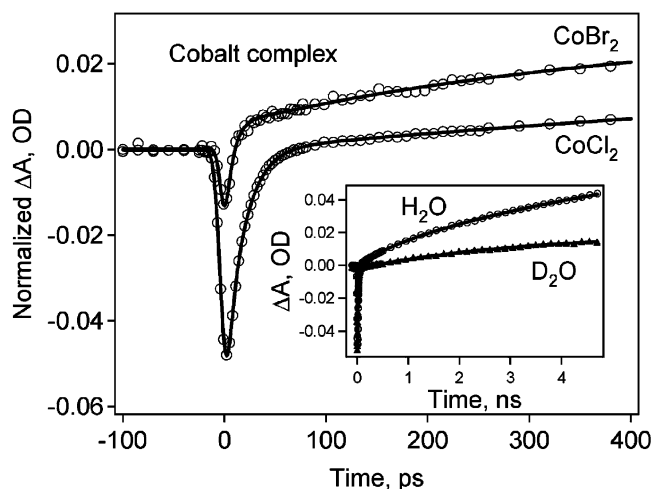
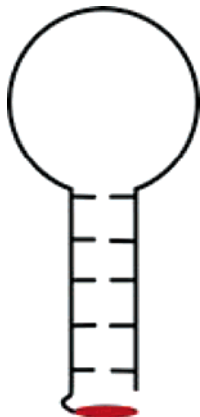


Figure 3. Transient absorption of ligand substitution reactions of the $[\text{CoX}_2(\text{H}_2\text{O})_4]^{2-}$ system ($X = \text{Cl}^-$ or Br^-), induced by the T-jump: (○) experimental data, 660 nm; (—) theoretical fits with a multiexponential model convoluted with a Gaussian response function. Inset: long time dynamics of the cobalt complex in (○) pure H_2O and (▲) $\text{D}_2\text{O}:\text{H}_2\text{O} \cong 70:30$.

on the $\text{D}_2\text{O}/\text{H}_2\text{O}$ ratio. Thus such studies separate the heating through water from that of direct complex absorption at $\sim 1.45 \mu\text{m}$.

Our interests in biological studies have so far been on protein folding and DNA melting. For the latter, we studied a hairpin DNA, but synthesized to have a dye probe at the end (Scheme 3).¹⁸ We

Scheme 3. The Dye-Labeled DNA Hairpin



examined the effect of T-jump (Figure 4) and in two regimes: high and low ionic strength. We can clearly observe the ~ 20 ps dynamics at temperatures below the melting of DNA ($\sim 60^\circ\text{C}$, high salt solution; $\sim 30^\circ\text{C}$, low salt solution). This reflects the initial step of “local melting” prior to the full separation,¹⁹ normally characterized at steady state temperatures. The results imply significant dynamic mobility, which is faster than that inferred from NMR studies, in the melting process. Clearly, characterization of the dynamics along the path of melting and at different times is of interest to us.²⁰

In conclusion, we have developed an ultrafast T-jump method, which heats the water by up to 20°C and at the limit of water

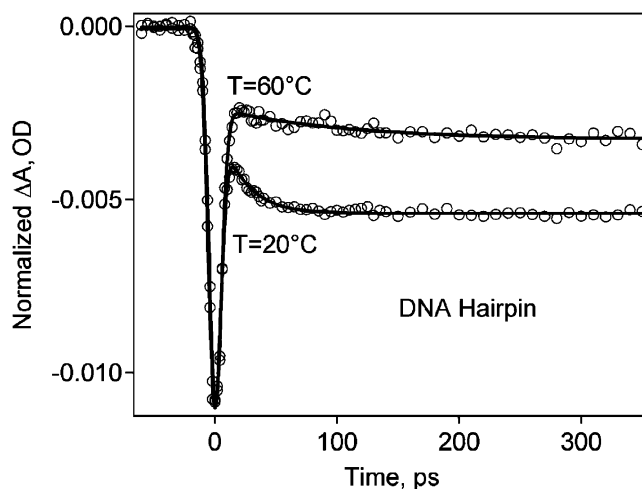


Figure 4. Transient absorption of DNA hairpin “local melting”: (○) experimental data; (—) theoretical fits with a multiexponential model convoluted with a Gaussian response function.

thermalization time (picosecond). The example given here shows the importance of separating events on the ultrashort time scale for solvation, conformation changes, and reactions. We demonstrate the application for molecular association, water exchange reactions, and DNA premelting dynamics. Many more systems are amenable for such ultrashort T-jump studies, including protein folding.

Acknowledgment. The research is supported by the National Science Foundation.

References

- (1) Eigen, M.; De Maeyer, L. D. Relaxation methods. In *Technique of Organic Chemistry*; Friess, S. L., Lewis, E. S., Weissberger, A., Eds.; Interscience: New York, 1963; Vol. 8, pp 895–1054.
- (2) Gruebele, M. C. *R. Biologies* **2005**, *328*, 701–712 and references therein.
- (3) Callender, R.; Dyer, R. B. *Curr. Opin. Struct. Biol.* **2002**, *12*, 628–633 and references therein.
- (4) Dyer, R. B.; Gai, F.; Woodruff, W. H.; Gilman, R.; Callender, R. *Acc. Chem. Res.* **1998**, *31*, 709–716.
- (5) Phillips, C. M.; Mizutani, Y.; Hochstrasser, R. M. *Proc. Natl. Acad. Sci. U.S.A.* **1995**, *92*, 7292–7296.
- (6) Chen, S.; Lee, I. Y. S.; Tolbert, W. A.; Wen, X. N.; Dlott, D. D. *J. Phys. Chem.* **1992**, *96*, 7178–7186.
- (7) Graener, H.; Ye, T. Q. *J. Phys. Chem.* **1989**, *93*, 5963–5965.
- (8) Steinel, T.; Asbury, J. B.; Zheng, J. R.; Fayer, M. D. *J. Phys. Chem. A* **2004**, *108*, 10957–10964.
- (9) Lock, A. J.; Woutersen, S.; Bakker, H. J. *J. Phys. Chem. A* **2001**, *105*, 1238–1243.
- (10) Arbeloa, F. L.; Gonzalez, I. L.; Ojeda, P. R.; Arbeloa, I. L. *J. Chem. Soc., Faraday Trans. 2* **1982**, *78*, 989–994.
- (11) Selwyn, J. E.; Steinfeld, J. E. *J. Phys. Chem.* **1972**, *76*, 762–774.
- (12) Dare-Doyen, S.; Doizi, D.; Guilbaud, P.; Djedaini-Pilard, F.; Perly, B.; Millie, P. *J. Phys. Chem. B* **2003**, *107*, 13803–13812.
- (13) Eisenthal, K. B. *Acc. Chem. Res.* **1975**, *8*, 118–123.
- (14) Hinckley, D. A.; Seybold, P. G.; Borris, D. P. *Spectrosc. Acta Part A: Mol. Biomol. Spectrosc.* **1986**, *42*, 747–754.
- (15) Adhikari, R.; Saha, S. K. *Z. Phys. Chem.: Int. J. Res. Phys. Chem. Chem. Phys.* **2005**, *219*, 1373–1384.
- (16) Kurnikova, M. G.; Balabai, N.; Waldeck, D. H.; Coalson, R. D. *J. Am. Chem. Soc.* **1998**, *120*, 6121–6130.
- (17) Magini, M. *J. Chem. Phys.* **1981**, *74*, 2523–2529.
- (18) Heinlein, T.; Knemeyer, J. P.; Piester, O.; Sauer, M. *J. Phys. Chem. B* **2003**, *107*, 7957–7964.
- (19) Klevan, L.; Armitage, I. M.; Crothers, D. M. *Nucleic Acids Res.* **1979**, *6*, 1607–1616.
- (20) Work to be published with Dr. Aiguo Wu.

JA0613862